Influence of transport Layer on Transient Suction Distribution in a Two-Layered Slope

Gambo Haruna Yunusa, Azman Kassim*, Ahmad Safuan A. Rashid
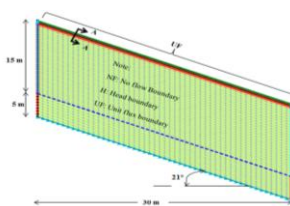
Department of Geotechnics and Transportation, Faculty of Civil Engineering, Universiti Teknologi Malaysia, 81310 UTM Johor Bahru, Johor Malaysia

*Corresponding author: azmankassim@utm.my

Graphical abstract

Abstract

Residual soil slope failure due to rainfall infiltration is one of geotechnical hazards receiving much attention in many tropical climate countries. The infiltrating water eliminates matric suction in the residual soil slope and results in slope failure. A capillary barrier is used to prevent excessive rainfall infiltration and preserve matric suction in the residual soil slope and hence prevent rainfall-induced slope failure. A numerical study to examine the performance of a transport layer in a two-layered slope using capillary barrier principle was presented in this paper. Material properties of tropical residual soils consisting of Grade V (silty gravel) and Grade VI (sandy silt) were used and modelled a two-layered slope. These material properties were obtained from representative soil sample of Balai Cerapan slope in Universiti Teknologi Malaysia, Johor Bahru campus. A granite chips (Gravel) was also incorporated to act as a transport layer in the numerical model. The simulated slope model was then subjected to three different rainfall intensities of 9 mm/h (rainfall 1), 22 mm/h (rainfall 2) and 36 mm/h (Rainfall 3) representing short, medium and high intensity rainfalls, respectively. A total of six numerical schemes were performed by restricting the thickness of the transport layer to 0.1 m. However, to assess the effect of the transport layer thickness on suction distribution; the thickness was increased to 0.2 m. The results of the study show that inclusion of gravelly transport layer enables the top layer of fine sandy silt residual soil to retain the infiltrating water as a result of capillary break developed at the interface and also divert it above the interface towards the direction of the toe of the slope. Similarly the transport layer is found to be effective in preventing water breakthrough occurrence into the underlying coarser soil layer of the two-layered slope, especially when the thickness of the transport layer is optimum.

Keywords: Slope failure, rainfall infiltration, capillary barrier, transport layer

■1.0 INTRODUCTION

Rainfall-induced slope failure is one of the most common and frequent natural disasters that occur frequently in tropical areas covered by residual soils and experienced periods of intense or prolong rainfall events [1-4]. Therefore, infiltration of rainwater into initially unsaturated residual soil is conceived as the most significant triggering factor to slope instability in tropical climate countries of the world [5-10]. This type of failure normally occurs above the ground water table with the orientation of the slip failure parallel to the slope surface, especially in areas where a residual or colluvial soil profile has formed over a bedrock interface [11, 12]

Rainfall-induced slope failure may occur as shallow or deep-seated slope failures. In general a high intensity and short duration rainfall usually triggers shallow slope failures, while a moderate intensity and long duration rainfall is responsible for deep-seated slope failure [13-16].

The water table in unsaturated residual soil slope is relatively deep. The matric suction above the water table provide additional shear strength to the unsaturated residual soil slope. However, the moisture content of the unsaturated residual soils increases as a result of rainfall infiltration into the unsaturated zone of the soil slope resulting in decreasing the negative pore-water pressure (matric suction) and subsequently the additional shear strength which is provided by the matric suction and trigger slope failure [2, 5, 17-20].

Despite the tremendous effort employed to curtail the menace of rainfall-induced slope failure, it is still a reoccurring natural hazard in many countries almost every year and usually resulted in loss of lives and causes considerable property damages. For instance, Hulu Kelang area in Malaysia is known to be a landslide-prone area. From 1993 to 2011 a total of 21 landslides which were triggered by rainfall were recorded in this area. These landslides resulted in death of more than 65 people and a considerable economical loss of more than RM245 million [21]. In 2004, Shikoku in Japan experienced many landslides which were triggered by typhoon rainfalls and faced huge losses of lives and properties. Similarly, Kagawa, the northeastern prefecture of Shikoku, was also hit by four typhoons in the same year which also resulted in landslides that causes loss of lives and properties [22]. During the 1951–1989 periods, Li and Wang [23] conservatively estimated more than 5000 death resulting in an

average of more than 125 deaths annually and an annual economic loss of about $500 million as a result of different landslides in China. The 1982 landslide in San Francisco which was also triggered by rainfall infiltration killed 25 people and caused more than $66 million in damage [9].

In recent years the use of capillary barrier principle is employed as a practical solution of preventing unsaturated residual soil slope against rainfall-induced slope failure [16, 24-28]. A capillary barrier is an earthen cover system consisting of fine-grained soil layer overlying a coarse-grained soil layer. The principle of capillary barrier relies on the properties of hydraulic conductivity as a function of pressure potential [29]. The contrast in particle sizes between the fine and coarse grained soil layers results in difference in hydraulic properties and permeability function) of the soil across the fine-coarse soil interface [30]. The infiltrated water into a capillary barrier system is stored in the fine-grained soil layer by capillary forces and is eventually remove by evaporation, evapotranspiration or by lateral drainage. However, when there is significant inflow into the system, the capillary forces ceases and the fine-grained layer can no longer retain the accumulated water which eventually results in significant inflow of water into the underlying coarse-grained layer, and the matric suction at the interface is called breakthrough suction. There are two ways of determining breakthrough suction as suggested by previous researchers: According to Parent and Cabral, [31] and Ross [29]; breakthrough suction is the matric suction at which the hydraulic conductivity curves of the two soils intersect. While Stormont and Anderson [32] and Tami, *et al.* [27] suggested that breakthrough suction is the water entry value of the coarse-grained soil.

The use of capillary barrier as a soil cover for landfills and waste containment has been study extensively (e.g. Khire *et al.*, [33]; Morris and Stormont, [34, 35]; Stormont, [36, 37]). Similarly, the principle of capillary barrier has been extended to rainfall-induced slope failure to reduce the amount of rainfall infiltration into the unsaturated soil zone thereby maintaining the negative pore-water pressure and hence maintaining the additional shear strength provided by the matric suction and prevent or reduce the severity of rainfall-induced slope failure [25-28]. Various combinations of different materials were suggested for capillary barrier construction for preventing rainfall infiltration. Krisdani *et al.* [38] constructed a capillary barrier in a 2-D infiltration box to study the effectiveness of using residual (cohesive) soil as fine-grained soil layer and gravelly sand as coarse-grain soil layer and found out that capillary barrier existed in the constructed model when residual soil was used as fine-grained soil layer. Similarly, Krisdani *et al.* [39] investigated the use of geosynthetic material as coarse-grained layer using 1-D capillary barrier model and found that the geosynthetic material was more effective as coarse-grained layer than the common gravelly sand used, even though both material were able to create a capillary break which prevents breakthrough occurrence in a capillary barrier system.

The use of capillary barrier for slope protection has been study extensively; for example, Tami, *et al.* [27, 28] developed a physical sloping capillary barrier model to study the mechanism and effectiveness of capillary barrier in slope protection. Rahardjo, *et al.* [26] constructed and instrumented a capillary barrier system on a slope that experienced a shallow failure and found that that a capillary barrier system can effectively minimize rainfall infiltration into a slope.

One of the challenges in the use of capillary barrier principle in rainfall-induced slope failure is the occurrence of breakthrough especially during wet period when the soil slope experienced minimum suction, and normally the amount of infiltration is greater than the storage capacity of the fine-grained soil during wet period; and hence the fine-grained soil layer approaches saturation and breakthrough into the coarse-grained layer can easily occur [34]. The occurrence of breakthrough renders the system ineffective. To minimize or reduce the possibility of a breakthrough occurrence, Morris and Stormont [35] and Stormont and Morris [40] proposed the use of an unsaturated drainage layer (transport layer); which is an additional layer of different soil material of high permeability constructed above the interface of fine-grained and coarse-grained soil layers so that the infiltrating water can flow within this layer due to the sloping surface. A transport system is found to be more effective with unsaturated drainage layer by preventing the development of positive pore water pressure in response to rainfall infiltration.

This paper evaluate the performance of a transport layer placed in between the fine and coarse grained soil layers in a two-layered slope in diverting infiltrating water before breakthrough occurs when the system is subjected to different hydrological conditions.

■2.0 MATERIAL AND METHODS

Infiltration of rainwater into unsaturated residual soil slope eventually eliminates matric suction and consequently the apparent shear strength provided by the matric suction which can trigger slope failure. Gravelly materials classified as uniformly graded gravel (GP_u) were used to study the influence of transport layer in diverting the infiltrated water in a two-layered slope. The two-layered slope consists of Grade V (completely weathered rock) and Grade VI (residual soil) according to the six-grade rock weathering classification of International Society for Rock Mechanics, ISRM [41]; the materials are classified as silty gravel of high plasticity (GMH) and sandy silt of high plasticity (MHS) using British Standard Soil Classification System. These materials are used and modelled as a two-layered soil slope with transport layer using a finite element commercial software; Seep/W [42]. The soil input parameters used in modeling the two-layered slope and the slope geometry were obtained from a Balai Cerapan slope (Figure 1). It is a sloping site located between latitude 1°34'11"N and Longitude 103°38'40"E within Johor Bahru campus of Universiti Teknologi Malaysia. From the appearance and geometry of the slope, it appeared to be a uniform cut slope with approximate slope angle of 21°. The height and length of the slope are approximately 17 m and 47 m, respectively.
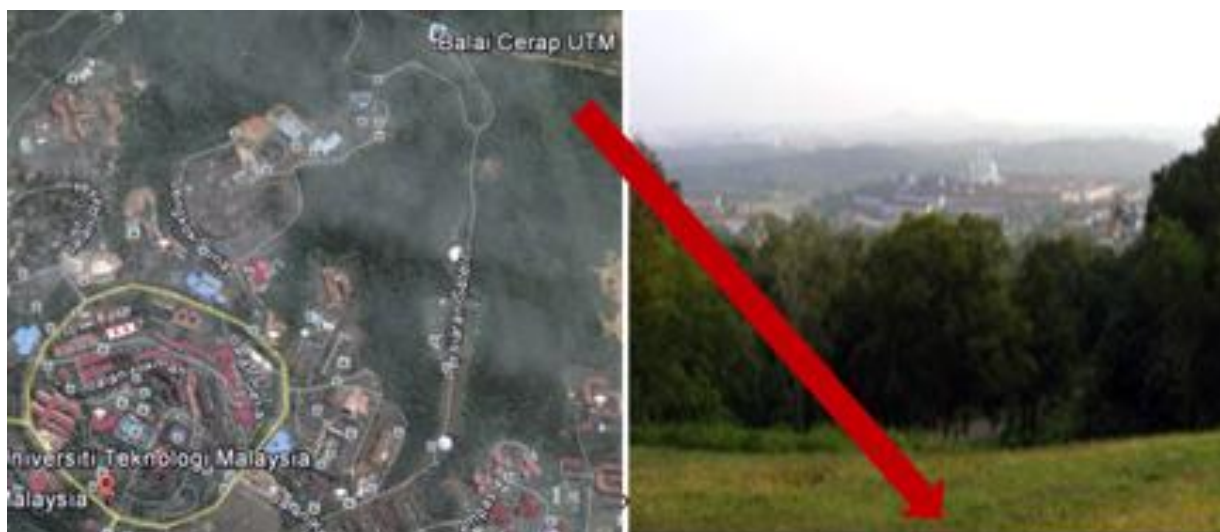
Figure 1 Location of Balai Cerapan Slope, UTM, Johor Bahru campus

To determine the required soil input parameters; representative soil samples were collected for laboratory soil testing. Grade VI residual soil sample was obtained from the first 0.5 m depth from the ground surface and Grade V was obtained from 0.5 m to 1.5 m depth. These soil samples were then subjected to various laboratory tests for the determination of indexes, engineering and hydraulic properties.

The index tests conducted include particle size distribution, atterberg limits and specific gravity tests. These tests were conducted based on recommended procedures outlined in BS 1337: Part 2 [43]. The engineering property tests conducted include compaction, shear strength and permeability tests. The compaction test was conducted based on recommended procedures outlined in BS 1337: Part 4 to determine the maximum dry density and optimum moisture content of the samples. Consolidated Isotropic Undrained (CIU) triaxial test and shear box tests were also conducted on these soil materials to determine the total and effective shear strength characteristics of the soils based on recommended procedures outlined in BS 1337: Part 8 and part 7, respectively. To determine the saturated coefficient of permeability of the materials, standard and modified constant-head and falling head permeability tests were used. The constant-head permeability test was carried out to determine k_{sat} for the gravel based on recommended procedure outlined in BS 1337: Part 5. The procedure outlined by Head and Epps [44] was used to determine k_{sat} of the fine-grained soil materials (Grade VI) using falling-head permeability test. While the modified constant head test was employed for the coarse-grained (Grade V) soils. The

important hydraulic properties of the materials are the SWCC and unsaturated hydraulic conductivity. The SWCC was obtained using pressure plate test conducted with pressure plate equipment using recommended procedure outlined in ASTM: D6836-02 ASTM [45]. The unsaturated hydraulic conductivity functions of these materials were estimated from their SWCCs using van Genuchten [46] method, as recommended by Leong and Rahardjo [47].

The summary of the basic and hydraulic material properties obtained from the laboratory tests are presented in Tables 1 and 2, respectively. Similarly, the grain-size distribution, the SWCC and the hydraulic conductivity functions of these materials are also presented in Figures 2, 3 and 4, respectively.

The breakthrough suction used in this study was determined using the method outlined by Parent and Cabral [31] and Ross [29]. It is taken as the suction at the intersection of the soil hydraulic conductivity curves. As shown in Figure 4; the breakthrough suction for the sandy silt - silty gravel and gravel - silty gravel are 4.5 kPa and 1.5 kPa, respectively.

The typical soil arrangement of Balai Cerapan slope is in such a way that the grade VI residual soil existed on top of the grade V of completely weathered rock. This typical soil arrangement (shown in Figure 5) was obtained from Kassim [48] and it conformed to the typical weathering classification as reported by Little [49].

Table 1 Basic properties of the materials used in the study

Description	Sandy Silt	Silty Gravel	Gravel
British Soil Classification system	MHS	GMH	GPu
Liquid limit, w_L (%)	59.3	53.2	-
Plastic Limit, w_P (%)	31.9	35.5	-
Plasticity Index, PI	27.4	17.7	-
Moisture content, w (%)	32	32	-
Specific gravity, G_s	2.65	2.63	2.68
Saturated Coefficient of Permeability, k_{sat} (m/s)	5.00×10^{-7}	3.68×10^{-6}	3.46×10^{-2}

Table 2 Hydraulic properties of the materials

Description	Sandy Silt	Silty Gravel	Gravel
Saturated Volumetric water content, θ_s (m^3/m^3)	0.45	0.41	0.37
Residual water content, θ_r (m^3/m^3)	0.34	0.28	0.03
Residual matric suction, ψ_r (kPa)	32	23	0.8
Air-entry value, A_{ev} (kPa)	7	3.5	0.16
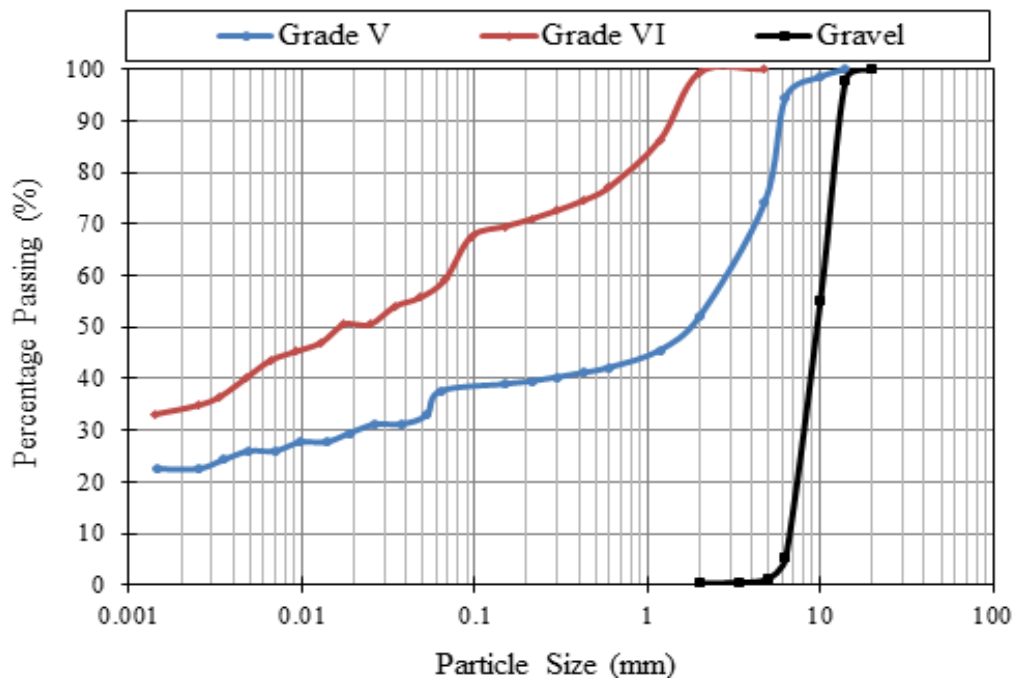
Figure 2 Particle Size Distribution curves for Grade V, Grade VI and gravel
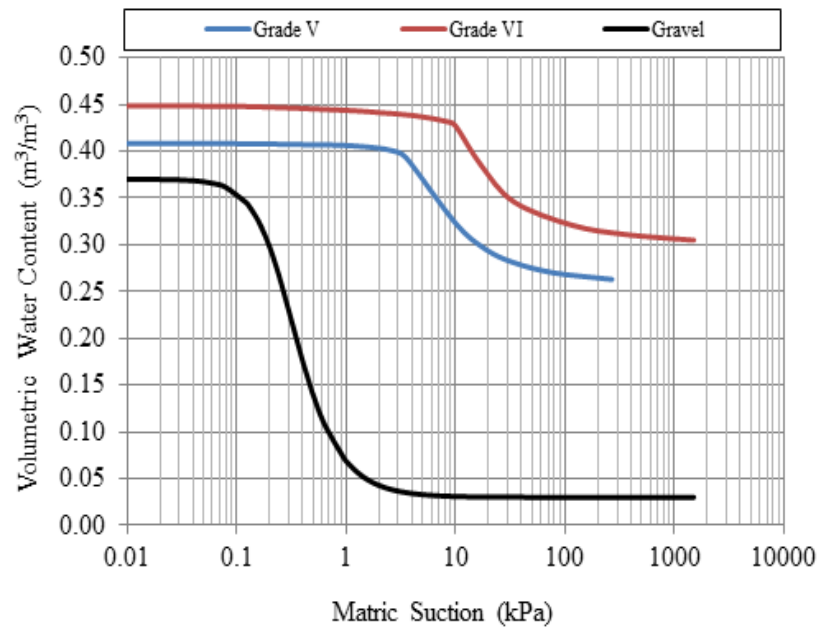
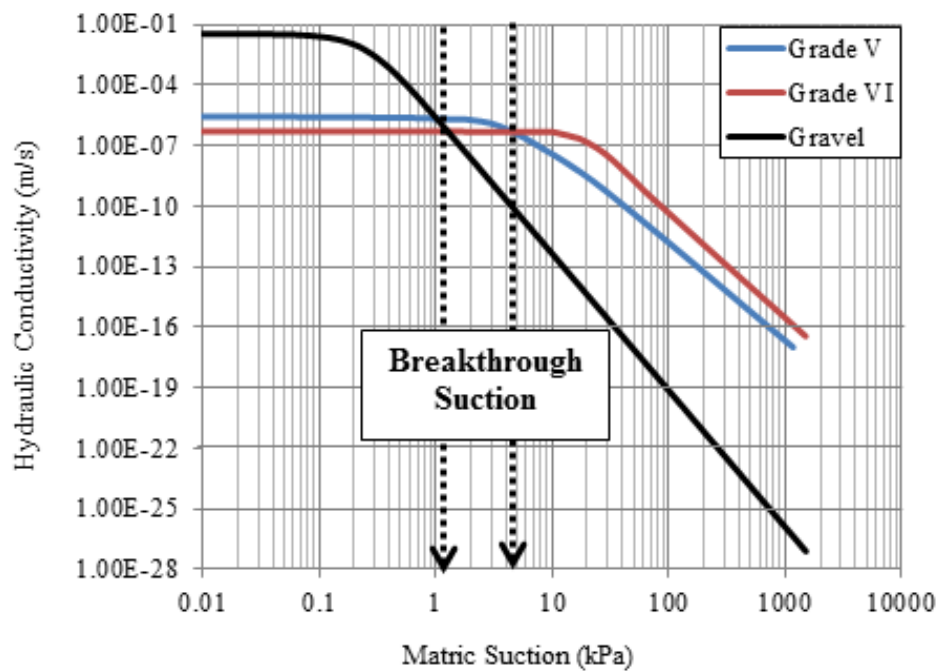**Figure 3** Soil Water Characteristics Curve (SWCC) for Grade V, Grade VI and gravel

Figure 4 Hydraulic conductivity functions for Grade V, Grade VI and gravel
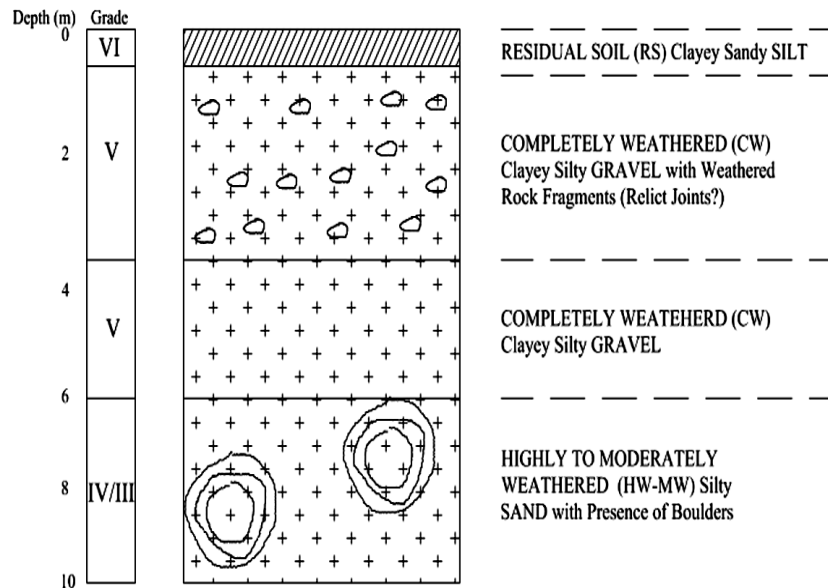
Figure 5 Typical soil arrangements in Balai Cerapan Slope

2.1 Numerical Modelling

The numerical modeling was carried out using SEEP/W [42] with the input of the basic and the hydraulic properties of the tested soil materials. The simplified slope model geometry as presented in Figure 6 consists of horizontal length of 30 m inclined at an angle of 21°. The modelled sloping length was shorter than the actual length of the slope at Balai Cerapan (i.e. 47 m) but this length is deemed to minimize the boundary effect as suggested by Kassim [48].

Due to the inherent weathering processes as a result of high temperature and intense rainfall intensity; the thickness of grade VI residual soil is small compared to other layers; therefore 0.3 m was modelled as the thickness of top grade VI residual soil. This assumption was supported by data obtained from previous study in the study area by Kassim [48] and Lee [50]. The gravel layer as transport (unsaturated drainage) layer was modelled in between the grade V and grade VI residual soil interface for the purpose of water diversion before breakthrough into the second layer of the two-layered slope. The thickness of this layer was considered as 0.1 to 0.2 m. While the silty gravel, was modelled as 0.3 m thick below the transport layer to complete the capillary barrier system. Similarly, a soil underlying the silty gravel was also assumed to be of the same material properties with the silty gravel.

The seepage model comprised of 4794 nodes and 4646 quadrilateral mesh elements to simulate the two-layered slope. Very fine quadrilateral elements (0.1 m 1 m) were designed for the top sandy silt layer. Fine quadrilateral elements ([0.1 m/0.2m] x 1 m) were designed to represent the transport layer. Fine quadrilateral elements (0.15 m x 1m) were designed to represent

the 0.3 m thick coarse silty gravel layer and finally large quadrilateral elements (0.5 m x 1 m) were used below silty gravel layer. Water table was located at 15 m below the ground surface to provide sufficient depth of unsaturated residual soil above water table. Three boundary conditions were assigned to the slope model as shown in Figure 6. The left and right edges above the water table were specified as a no flow boundaries ($Q = 0$), while the edges below the water table were assigned as head boundaries with pressure head equal to the vertical distance from the datum to the water table. These boundary conditions enhance the lateral flow to occur within the saturated/unsaturated zone. Finally, the top boundary was modelled as flux boundary with applied flux equal to the rainfall intensity.

Prior to the transient seepage analysis; several analyses were conducted to simulate the initial conditions of the soil prior to the rainfall event. The analyses were stopped when the suction values obtained is approximately equal to the value of suction at residual water content of the SWCC. This assumption was supported by other studies such as Gofar and Lee [51]; Kassim, [48]; Lee *et al.* [52]; Lee [50] and [53].

The complete sysem was then subjected to three different rainfall intensities of 9 mm/h, 22 mm/h and 36 mm/h designated as rainfall 1, rainfall 2 and rainfall 3, respectively. The duration of the rainfall events were restricted to 24 hours, however, the analyses periods was extended to 48 hours so as to observe the effect of infiltrating water after a particular rainfall event. Similar rainfall intensities were used by Li*, et al.* [16] and Rahardjo *et al.* [54] to study the effect of cover with capillary barrier effect in South China and the effects of groundwater table position and soil properties on stability of slope during rainfall respectively.
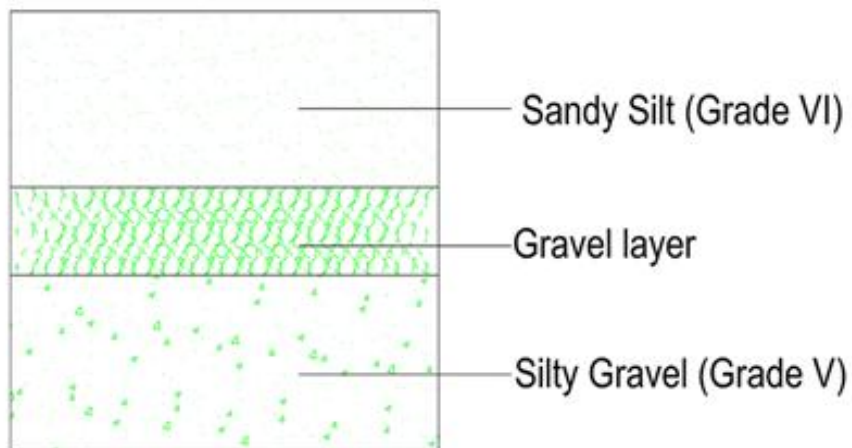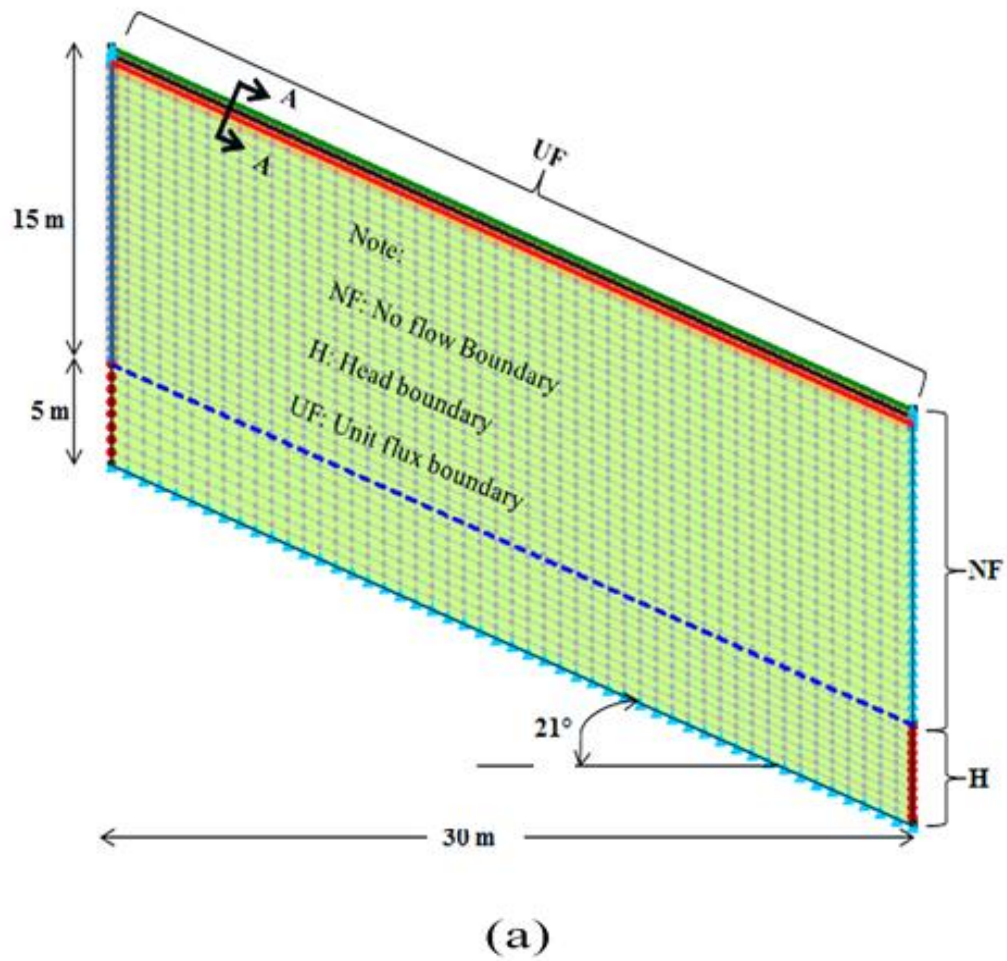
(a)

(b)

Figure 6 (a) Simulated slope model (b) Section A-A

The numerical modeling carried out in this study was parted into six different schemes (Scheme 1 to Scheme 6) as presented in Table 3. The thickness of the transport layer was restricted to 0.1 m throughout these schemes of the numerical modeling. However, to study the effect of the transport layer thickness on suction distribution; the thickness of the transport layer was later changed to 0.2 m in separate analyses. Hence, the obtained result was compared to that of 0.1 m thickness transport layer.

Table 3 Schemes of the Numerical Modeling used in the study

Numerical Scheme	Configuration	Rainfall
1	Two-layered slope without transport layer	1
2	Two-layered slope with transport layer	1
3	Two-layered slope without transport layer	2
4	Two-layered slope with transport layer	2
5	Two-layered slope without transport layer	3
6	Two-layered slope with transport layer	3

■3.0 RESULTS AND DISCUSSIONS

The results obtained from this study were presented in terms of pore water pressure (kPa) and time (hour) to obtain the approximate time at which breakthrough occurs in the system. This enables the performance of the two-layered slope with transport layer to be directly assessed. Three different locations (i.e. the crest, the middle and the toe of the slope) were chosen to investigate the pore water pressure distribution in the system.

3.1 Transient Suction Distribution For Scheme 1 And Scheme 2

The changes of the pore water pressure with time due to Scheme 1 and Scheme 2 at the interface of the crest, middle and toe of the two-layered slope are shown in Figure 7. The patterns of changes of the pore water pressure at these selected positions in a two-layered slope with and without transport layer are completely different.

In a two-layered slope without additional transport layer in between the grade V and grade VI residual soil the pore water pressure increases quickly at the initial stage of the rainfall and the suction at the interface of the two soil layers reaches breakthrough suction at approximately two different time intervals with the pore water pressure at the middle and the toe of the slope reaching breakthrough suction at the same time, while the pore water pressure at near the crest of the slope reaching the breakthrough suction at different time. This occurred at 13th hour at the crest and 7th hour at the middle and the toe of the modelled slope. This shows that the infiltrating water accumulates above the interface of the two-layered slope for short period of time before the occurrence of breakthrough. This happened as a result of small variation in particle sizes between the two soil layers which results in small contrast in the hydraulic conductivity function of the two soil layers. As shown in Table 1, the saturated hydraulic conductivity between the two soil layers only varies within one order of magnitude. After the 24 hour rainfall duration the pore water pressure start to recover but at very slow pace in fact there was continuous movement of infiltrating water downward for more than 3 hours after the elapse of 24 hours rainfall duration. The pore water pressure at the crest of the slope falls below the breakthrough suction 12 hours after the rainfall have stopped. However due to significant inflow that occurred at the middle and near the toe of the slope the pore water pressure

only approaches the breakthrough suction at the end of the analyses period (i.e. 48 hours). The lag in time at which breakthrough occurred between the selected positions indicates that the infiltrating water moves from crest to the toe of the slope as a result of difference in elevation in the two-layered slope model.

In a two layered slope with additional transport layer in between the two soil layers, the pore water pressure was maintained at near the crest of the slope throughout the rainfall duration and analyses period which indicates that the infiltrating water was retained in the grade VI residual soil by capillary forces and flow above the interface of the transport layer and grave V silty gravel layer. This happens as a result of high capillary break developed between grade VI and gravel layer due to large particle size contrast between the two layers. Similarly, at breakthrough matric suction (i.e. 4.5 kPa); the difference between k of gravel (i.e. 10^{-10} m/s) and k of grade V (i.e. 10^{-6} m/s) was about 4 orders of magnitude.

Unlike in the case of two-layered slope without additional transport layer (scheme 1); the variation in the pore water pressure in the middle and the toe of the slope are completely different. At the middle of the slope the pore water pressure was maintained for 16 hours from the beginning of the rainfall event. The sudden decrease in suction at the middle of the slope below the breakthrough suction is anticipated because the system was able to successfully divert the infiltrating water which flows through the transport layer and the amount of water diverted increases from the crest towards the toe of the slope. The suction at these points redistributes and falls below the breakthrough suction instantaneously before the end of 24 hours rainfall duration; which really implies the temporary nature of the initial breakthrough that occurred.

At the toe of the slope the pore water pressure was also maintained for approximately 10 hours from the beginning of the rainfall event before the sudden drop in suction below breakthrough suction and up to a positive value of 7 kPa. This is anticipated because the infiltrating water was successfully diverted and flow above the interface. Even though this indicates breakthrough occurrence but it occurred as a result of diverted water that accumulates at the toe of the modelled two-layered slope before it drains out from the right-hand boundary. The drainage of water allows the pore water pressure to redistribute and fall below the breakthrough suction. This clearly shows a

significant improvement compared to the system without transport layer.

The direction of water movement in the two systems is shown in Fig. 8. It can be seen that the infiltrating water instantly moves downward and breakthrough the interface of the two soil layers in the two-layered slope without transport layer (Fig. 8*a*). However when the transport layer was included in between the

upper sandy silt and the lower silty gravel soil layers of the two-layered modelled slope; the infiltrating water was diverted along the interface (Fig. 8*b*) and a lateral flow appears above the interface of the transport layer and the silty gravel layer.
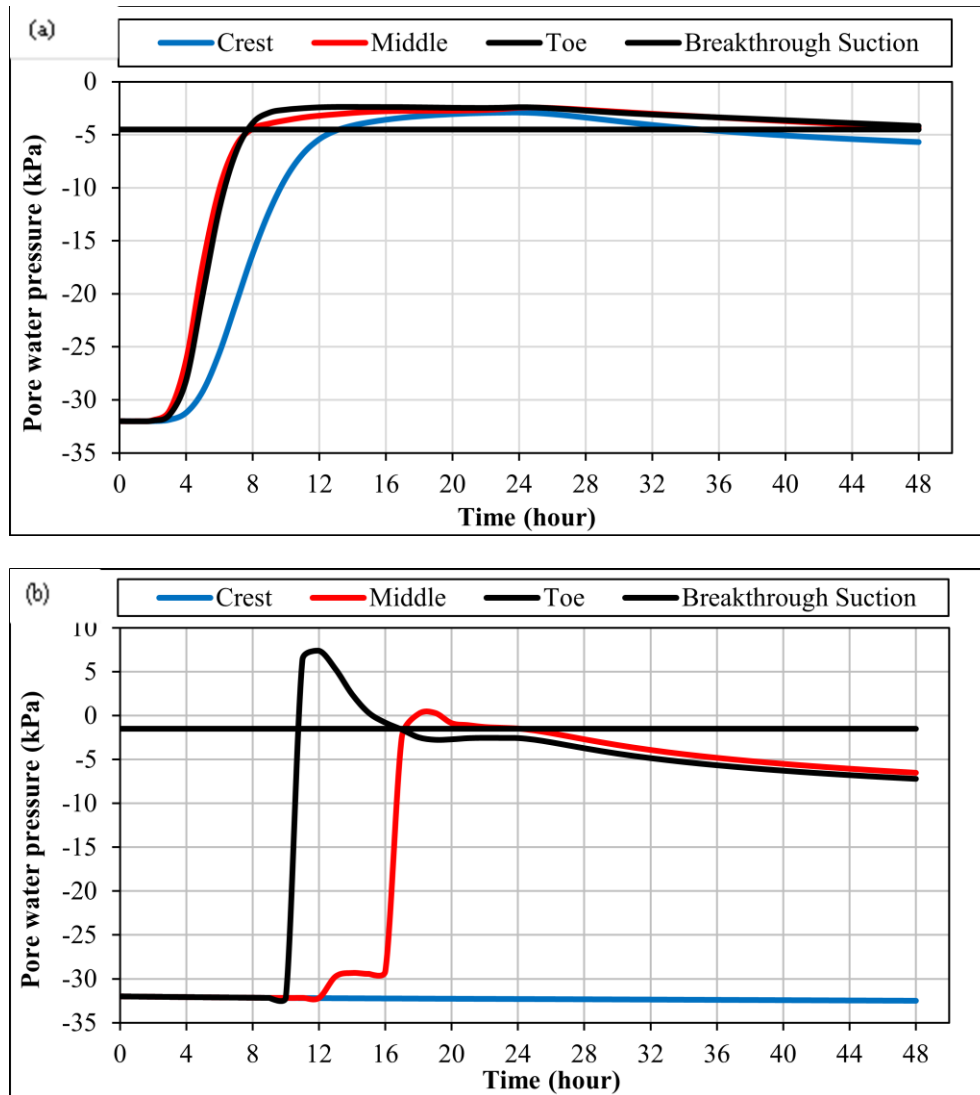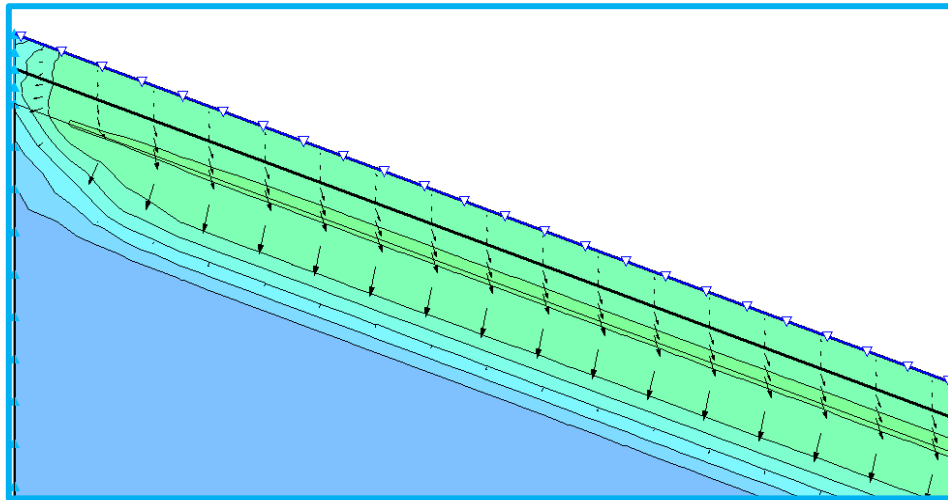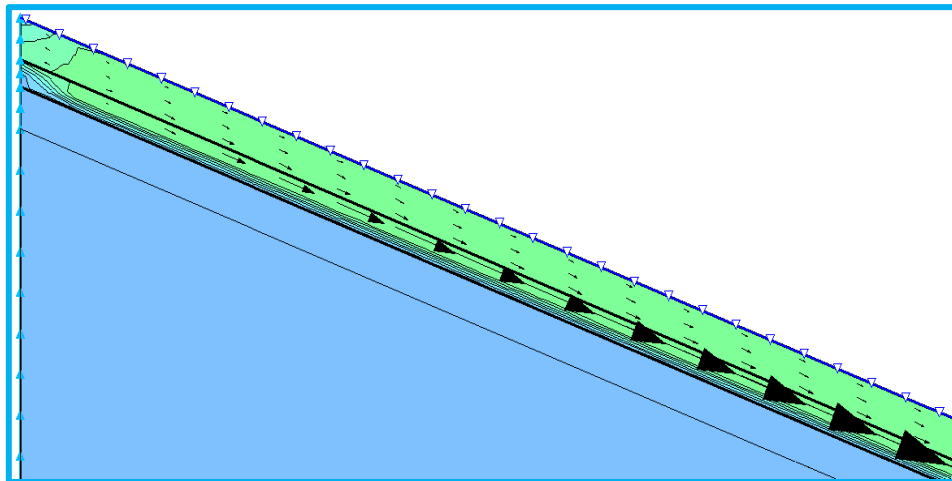

Figure 7 Variation of pore water pressure with time along the interface of the systems for scheme 1 (a) without transport layer (b) with transport layer

(a)

(b)

Figure 8 Direction of water movement (a) without transport layer (b) with transport layer

3.2 Transient Suction Distribution For Scheme 3 And Scheme 4

The changes in the pore water pressure for scheme 3 and scheme 4 at the three chosen positions (crest, middle and toe) are shown in Figure 9. In a two-layered slope without the additional transport layer, the variation of pore water pressure in scheme 3 was nearly similar to that of scheme 1. The major difference was the time at which the pore water pressure redistributes and fall below the breakthrough suction after the rainfall have stopped. Unlike in rainfall 1 the suction redistributes and falls below the

breakthrough suction 6 hours after the rainfall duration (i.e. 24 hour) in the crest and 13 hours after the rainfall in the middle and the toe of the slope. Similarly when the transport layer was included in the two-layered modelled slope the variation of the pore water pressure is also similar to that of scheme 2. However, the positive pore water pressure value at the toe of the slope is approximately twice that of scheme 2 which signifies that higher amount of water was diverted in the system due to higher rainfall intensity compared to rainfall 1 and the infiltrating water was also successfully diverted above the interface and accumulates at the toe of the slope than as in scheme 2.
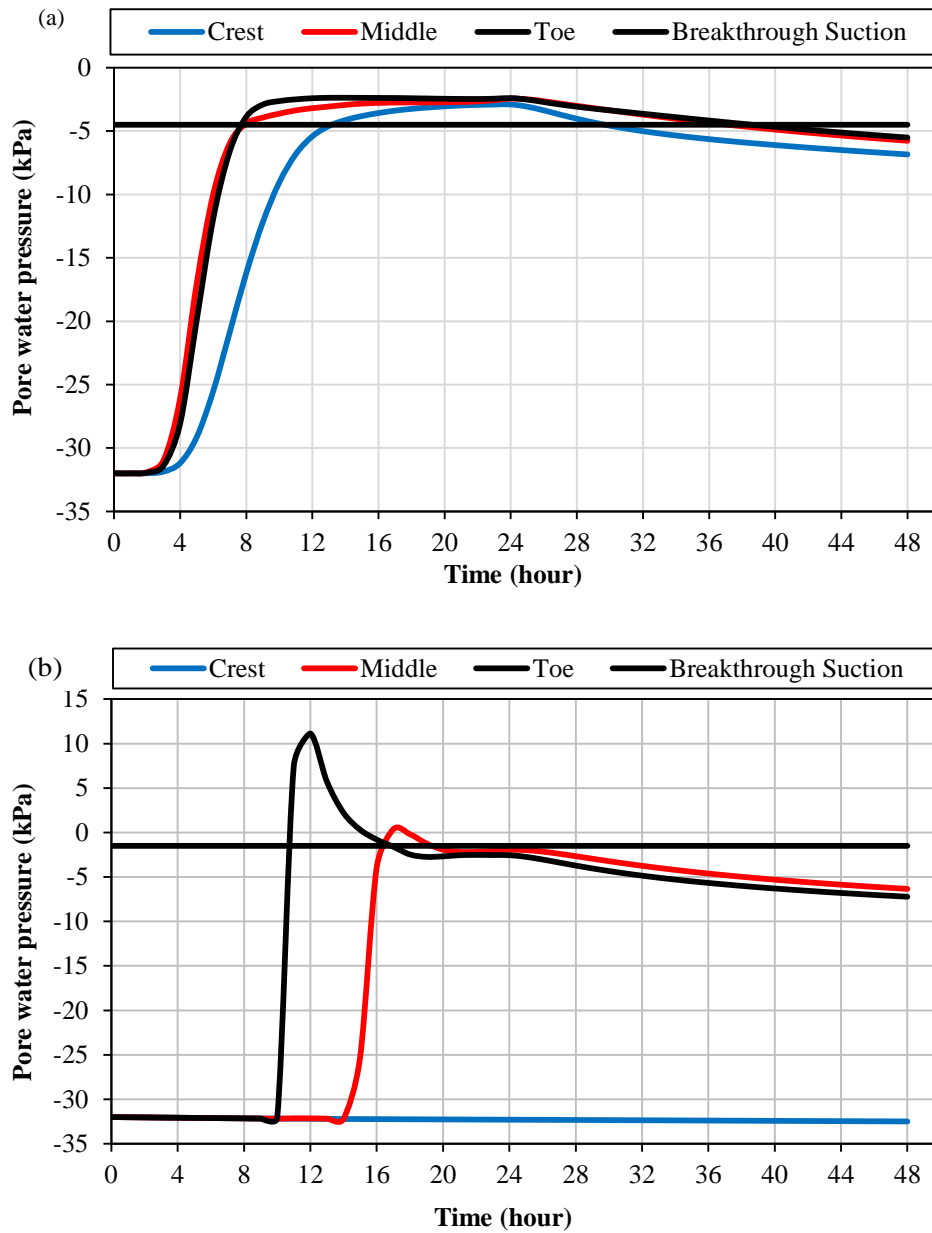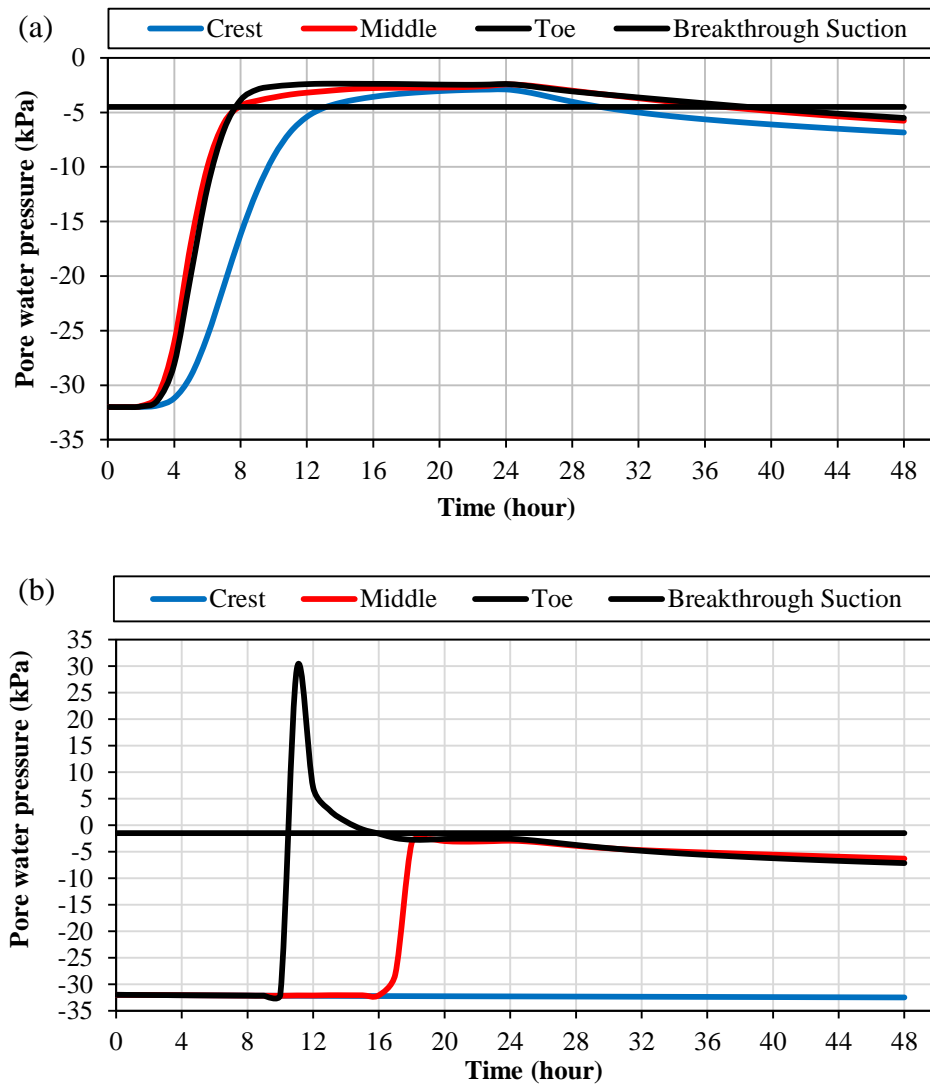
Figure 9 Variation of pore water pressure with time along the interface of the systems for scheme 2 (a) Without transport layer (b) with transport layer

3.3 Transient Suction Distribution For Scheme 5 And Scheme 6

The changes in the pore water pressure for scheme 5 and scheme 6 at the three chosen positions (crest, middle and toe) are shown in Figure 10. The changes in pore water pressure with time in a two-layered slope without additional transport layer for scheme 5 is similar to that of scheme 3 without any difference. The redistribution of suction also occurred at the same time as that scheme 3. However, when the additional transport layer was included in the two-layered slope the pore water pressure was maintained below breakthrough suction at the crest and middle of the slope. The positive pore water pressure at the toe of the slope increases significantly compared to scheme 4, in fact, it is almost three times that of scheme 4, which clearly shows that more water was diverted above the interface because in the increase in the amount of rainfall intensity in rainfall 3 than rainfall 2 and 1and the diverted water accumulates at the toe of the slope more in scheme 6 than in scheme 4 and scheme 2.

Figure 10 Variation of pore water pressure with time along the interface of the systems due to rainfall 3 (a) Without transport layer (b) with transport layer

3.4   Effect Of Transport Layer Thickness On Transient Suction Distribution

To evaluate the effect of transport layer thickness on suction distribution, the thickness of the additional transport layer in the simulated two-layered slope model was increased to 0.2 m and the changes in the pore water pressure distribution with time for the three rainfalls (rainfall 1, rainfall 2 and rainfall 3) were determined. Figure 11 shows the variation of pore water pressure at the crest, middle and toe of the modelled slope due the three rainfall intensities considered in this study. The pore water pressure at the crest of the slope is maintained throughout the rainfall durations and analyses period for all the three rainfalls considered. This shows that the infiltrating water is successfully stored in the sandy silt residual soil and was later diverted above the interface of the soil layers. However, there is variation in the pore water pressure distribution at the middle and the toe of the

slope for all the three rainfalls. As explained by Ross [29] the volume of water moving laterally increases in the down-dip direction as additional infiltration is diverted by the barrier. Therefore these variations in the pore water pressure at the middle and the toe of the slope is as a result of the increase in the volume of water diverted laterally. The pore water pressure at the middle and the toe of the slope were maintained throughout rainfall duration which shows that the maximum diversion was achieved with 0.2 m thickness of the additional transport layer. The transport layer is about 10 times coarser than the overlying layer (Figure 2).

This findings are in accordance with results obtained by Smesrud and Selker [55] which explained that when the underlying coarse material is 2.5 times coarser than the overlying fine material; 80% of the maximum diversion can be achieve and 90% can be achieved with coarse material which are 5 times coarser than the overlying fine material.
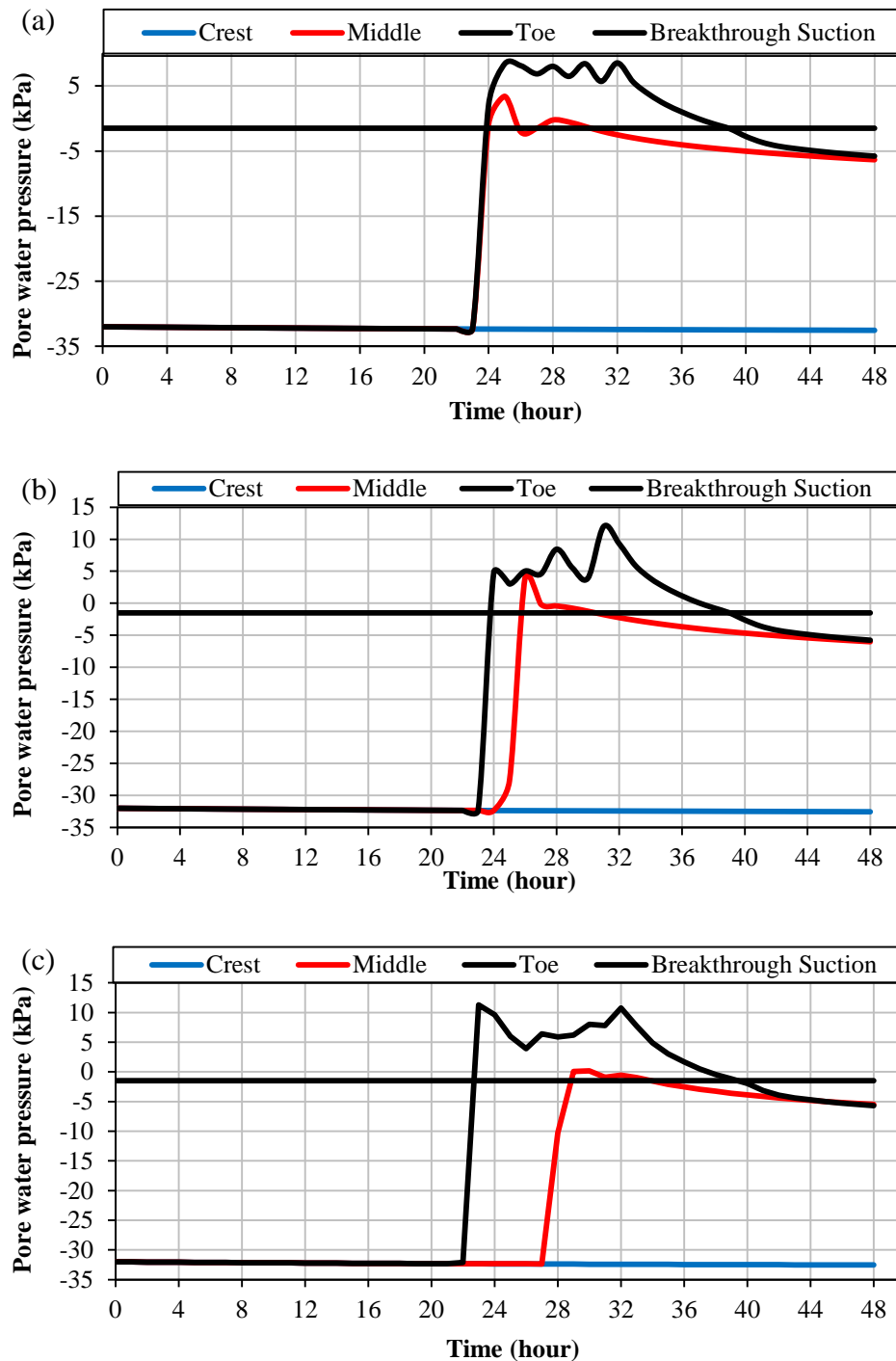
Figure 11 Variation of pore water pressure with time for 0.2 m thick transport layer (a) Rainfall 1- 9 mm/h (b) Rainfall 2- 22 mm/h (c) Rainfall 3- 36 mm/h

3.5 Comparison Of Suction Distribution Due To Transport Layer Thickness

The changes in the pore water pressure due to 0.1 m thick transport layer were compared to that of 0.2 m transport layer thickness as shown in Figure 12. To clearly explain the difference between the two thicknesses of the transport layer, the data shown in Table 3 were extracted from Figure 12. Variation in time to reach breakthrough suction at the crest, middle and toe of the

slope were shown in Table 3. The pore water pressure does not attain the breakthrough suction at the crest of the simulated slope model for both 0.1 m and 0.2 m transport layer thickness. However, the time to reach breakthrough suction for 0.1 m and 0.2 m transport layer thicknesses increases with the increase in rainfall intensity which clearly shows a significant improvement. But at the toe of the slope the time to reach breakthrough suction decreases with increase in rainfall infiltration because as rainfall increase more water is diverted above the interface which later

accumulates at the toe of the slope which resulted in total elimination of the matric suction at the toe of the slope.
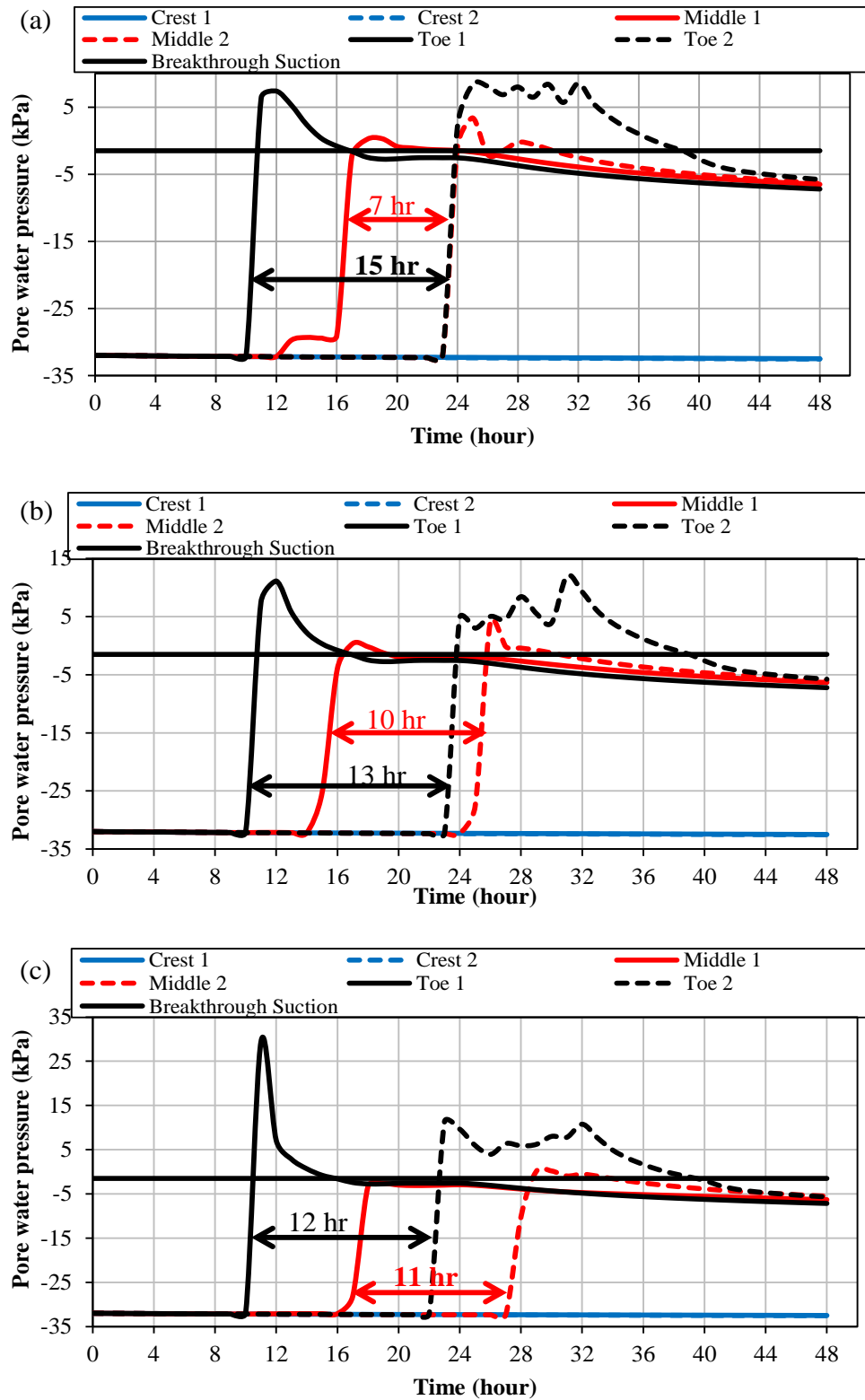

Figure 12 Comparison of pore water pressure variation with time for 0.1 and 0.2 m thick transport layer (a) Rainfall 1- 9 mm/h (b) Rainfall 2- 22 mm/h (c) Rainfall 3- 36 mm/h

Table 4 Comparison of time (in hour) to reach breakthrough suction between 0.1 m and 0.2 m transport layer

Rainfall Identity	Crest	Middle	Toe
Rainfall 1	-	7	15
Rainfall 2	-	10	13
Rainfall 3	-	11	12

3.6 Discussions

For a system of soils to work on the principle of capillary barrier effect there must be a contrast in the particle sizes between the two soil systems which eventually develops a capillary break at their interface and impedes breakthrough occurrence. The variation in particle sizes between the two soil layers results in different hydraulic conductivity between the soil layers. The more the contrast in the particle sizes the higher the variation in the hydraulic conductivity function and the higher the capillary break at the interface of the soil layers.

The performance of a capillary barrier system is significantly affected with continuous water infiltration into the system, especially during wet period when the soil condition is initially wet. This results in breakthrough occurrence which can trigger rainfall-induced slope failure. Inclusions of transport layer of coarser material assist in diverting the infiltrating water above the interface and transport it towards the toe of the slope. The thickness of transport layer play significant role in impeding breakthrough occurrence as shown in section 3.4 and section 3.5.

■4.0 CONCLUSIONS

This numerical study was conducted to investigate the performance of transport layer constructed in between a two-layered residual soil slope in diverting the infiltrating water before breakthrough occurrence. The system was subjected to three different rainfall intensities of 9 mm/h, 22 mm/h and 36 mm/h for a total duration of 24 hour while the analyses periods were extended to 48 hour to observe the process of suction redistribution after the rainfall duration elapsed. Based on the outcome of the study; the following conclusions can be drawn from the study.

(1) Capillary barrier effect exists in a two-layered residual soil slope consisting of grade V and grade VI residual soil. The weathering processes in the residual slope profile resulted in very fine material of shallow depth to be form above coarser material. However, this capillary barrier effect ceases within short period of time due to rainfall infiltration in the system as a result of small particle size contrast between the two soil layers.

(2) For all the three rainfall intensities and duration considered the infiltrating water was successfully diverted and flow above the interface in the downdip direction when a transport layer is included. However, the results show that the diversion length of the system may be less than 15 m because a temporary breakthrough occurs at the middle of the slope, even though the suction was redistributed later before the end of the rainfall duration.

(3) Higher capillary break is developed between the gravel and sandy silt layer which results in water diversion along the interface of the system and the higher the rainfall intensity the more water is diverted from the system before breakthrough occurs.

(4) The changes in suction is faster in the system without transport layer due accumulation of much water at the interface of the two soil layers and in the fine-grained layer before breakthrough occurs.

(5) Increase in thickness of transport layer increases the water diversion of the system as noticed when the thickness of the transport layer was increased from 0.1 m to 0.2 m.

■References

[1] Dai, F.C., C.F. Lee. and Y.Y. Ngai. 2002. Landslide risk assessment and management: an overview. *Engineering Geology*. 64(1): 65–87.

[2] Fourie, A.B. 1996. Predicting Rainfall-induced Slope Instability. *Proceedings of the Institution of Civil Engineers-Geotechnical Engineering*. 119: 211–218.

[3] Lumb, P. 1975. Slope failures in Hong Kong. *Quarterly Journal of Engineering Geology and Hydrogeology*. 8(1): 31–65.

[4] Wolle, C.M. and W. Hachich. 1989. Rain-induced landslides in southeastern Brazil. *Proceedings of the 12th International Conference on Soil Mechanics and Foundation Engineering*. 1639–1644.

[5] Au, S.W.C. 1998. Rain-induced slope instability in Hong Kong. *Engineering Geology*. 51(1): 1–36.

[6] Brand, E.W. 1984. Landslides in Southeast Asia: a State-of-the-art Report. *Proceedings of the 4th International Symposium on Landslides*. 17–59.

[7] Collins, B. and D. Znidarcic. 2004. Stability Analyses of Rainfall Induced Landslides. *Journal of Geotechnical and Geoenvironmental Engineering*.130(4): 362–372.

[8] Dai, F., C.F. Lee, and S. Wang. 1999. Analysis of rainstorm-induced slide-debris flows on natural terrain of Lantau Island, Hong Kong. *Engineering Geology*. 51(4): 279–290.

[9] Keefer, D.K., R.C. Wilson., R.K. Mark., E.E. Brabb., W.M. Brown., S. D. Ellen., E.L. Harp., G.F. Wieczorek., C.S. Alger. and R.S. Zatkin. 1987. Real-time Landslide Warning During Heavy Rainfall. *Science*. 238(4829): 921–925.

[10] Tsaparas, I., H. Rahardjo., D.G. Toll. and E.C. Leong. 2002. Controlling parameters for rainfall-induced landslides. *Computers and Geotechnics*. 29: 1–27.

[11] Cho, S. and S. Lee. 2002. Evaluation of Surficial Stability for Homogeneous Slopes Considering Rainfall Characteristics. *Journal of Geotechnical and Geoenvironmental Engineering*. 128(9): 756–763.

[12] Rahardjo, H., T.T. Lim., M.F. Chang. and D.G. Fredlund. 1995. Shear strength characteristics of a residual soil with suction. *Canadian Geotechnical Journal*. 32: 17.

[13] Aleotti, P.A. 2004. Warning system for rainfall-induced shallow failures. *Engineering Geology*. 73(3–4): 247–265.

[14] Iverson, R.M. 2000. Landslide triggering by rain infiltration. *Water Resources Research*. 36(7): 1897–1910.

[15] Leroueil, S. 2001. Natural slopes and cuts: movement and failure mechanisms. *Geotechnique*. 51(3): 197–243.

[16] Li, J.H., L. Du., R. Chen. and L.M. Zhang. 2013. Numerical investigation of the performance of covers with capillary barrier effects in South China. *Computers and Geotechnics*. 48(0): 304–315.

[17] Fredlund, D. G. and H. Rahardjo. 1993. *Soil Mechanics for Unsaturated Soils*: John Wiley & Sons, Inc.

[18] Fredlund, D.G., H. Rahardjo. and M.D. Fredlund. 2012. *Unsaturated Soil Mechanics in Engineering Practice*: John Wiley & Sons, Inc.

[19] Rahardjo, H., T.T. Lee., E.C. Leong. and R.B. Rezaur. 2005. Response of a residual soil slope to rainfall. *Canadian Geotechnical Journal*. 42(2): 340–351.

[20] Rahardjo, H., E.C. Leong., S.D. Michael., M.G. Jason. and S.K. Tang. 2000. Rainfall Induced Slope Failures. *Geotechnical Engineering Monograph 3, NTU-PWD Geotechnical Research Centre, NTU, Singapore*.

[21] Lee, M. L., K. Ng., Y. Huang. and W. Li. 2014. Rainfall-induced landslides in Hulu Kelang area, Malaysia. *Natural Hazards*. 70(1): 353-375.

[22] Dahal, R., S. Hasegawa., A. Nonomura., M. Yamanaka., T. Masuda. and K. Nishino. 2008. GIS-based weights-of-evidence modelling of rainfall-induced landslides in small catchments for landslide susceptibility mapping. *Environmental Geology*. 54(2): 311–324.

[23] Li, T. and S. Wang. 1992. Landslide hazards and their mitigation in China *Beijing: Science Press*.

[24] Harnas, F.R., H. Rahardjo., E.C. Leong. and J.Y. Wang. 2014. Experimental Study on Dual Capillary Barrier using Recycled Asphalt Pavement Materials. *Canadian Geotechnical Journal*. 10.1139/cgj-2013-0432.

[25] Rahardjo, H., E.C. Leong., A. Satyanaga., N.Y. Song., T.H. Tuan. and H.C. Juay. 2014. Rainfall-Induced Slope Failures and Preventive Measures in Singapore. *Geotechnical Engineering Monograph, NTU-HDB Research Collaboration, NTU, Singapore*.

[26] Rahardjo, H., V.A. Santoso., E.C. Leong., Y.S. Ng. and C.J. Hua. 2012. Performance of an Instrumented Slope Covered by a Capillary Barrier System. *Journal of Geotechnical and Geoenvironmental Engineering*. 138(4): 481–490.

[27] Tami, D., H. Rahardjo., E.C. Leong. and D.G. Fredlund. 2004. A Physical Model for Sloping Capillary Barriers. *Geotechnical Testing Journal*. 27(2): 16.

[28] Tami, D., H. Rahardjo., E.C. Leong. and D.G. Fredlund. 2004. Design and laboratory verification of a physical model of sloping capillary barrier. *Canadian Geotechnical Journal*. 41(5): 814–830.

[29] Ross, B. 1990. The diversion capacity of capillary barriers. *Water Resources Research*. 26(10): 2625–2629.

[30] Yang, H., H. Rahardjo., E.C. Leong. and D.G. Fredlund. 2004. A study of infiltration on three sand capillary barriers. *Canadian Geotechnical Journal*. 41(4): 629–643.

[31] Parent, S.-É. and A. Cabral. 2006. Design of Inclined Covers with Capillary Barrier Effect. *Geotechnical and Geological Engineering*. 24(3): 689–710.

[32] Stormont, J.C. and C. E. Anderson. 1999. Capillary Barrier Effect from Underlying Coarser Soil Layer. *Journal of Geotechnical and Geoenvironmental Engineering*. . 125(8): 641–648.

[33] Khire, M.V., C.H. Benson. and P.J. Bosscher. 2000. Capillary Barriers: Design Variables and Water Balance. *Journal of Geotechnical and Geoenvironmental Engineering*. 126(8): 695–708.

[34] Morris, C.E. and J.C. Stormont. 1997. Capillary Barriers and Subtitle D Covers: Estimating Equivalency. *Journal of Environmental Engineering*.123(1): 7.

[35] Morris, C.E. and J.C. Stormont. 1999. Parametric Study of Unsaturated Drainage Layers in a Capillary Barrier. *Journal of Geotechnical and Geoenvironmental Engineering*. 125(12): 1057–1065.

[36] Stormont, J.C. 1995. The effect of constant anisotropy on capillary barrier performance. *Water Resources Research*. 31(3): 783–785.

[37] Stormont, J.C. 1996. The effectiveness of two capillary barriers on a 10% slope. *Geotechnical & Geological Engineering*. 14(4): 243–267.

[38] Krisdani, H., H. Rahardjo. and E.C. Leong. 2005. Behaviour of Capillary Barrier System Constructed using Residual Soil. *Waste Containment and Remediation*. 1–15.

[39] Krisdani, H., E.C. Leong. and H. Rahardjo. 2006. Experimental Study of 1-D Capillary Barrier Model Using Geosynthetic Material as the Coarse-Grained Layer. *Unsaturated Soils 2006*. 1683–1694.

[40] Stormont, J.C. and C.E. Morris. 1997. Unsaturated Drainage Layers for Diversion of Infiltrating Water. *Journal of Irrigation and Drainage Engineering*. 123(5): 364–366.

[41] ISRM. 1981. Basic geotechnical description of rock masses (BGD). *International Journal of Rock Mechanics and Mining Sciences & Geomechanics Abstracts*. 18(1): 87–110.

[42] Geo-Slope International. 2007. *SEEP/W User's guide for finite element seepage analysis. Geo-Slope International Ltd*, Calgary, Alta.

[43] BSI. 1990. *Methods of Test for Soils for Civil Engineering Purposes (BS 1377:Part 1-9)*. Methods of Test for Soils for Civil Engineering Purposes (BS 1377:Part 1-9), British Standards Institution, London.

[44] Head, K.H. and R.J. Epps. 2011. *Manual of Soil Laboratory Testing: Permeability, Shear Strength and Compressibility Tests* Vol. 2, 3rd ed.: Whittles Publishing, CRC Press, Taylor & Francis group.

[45] ASTM. 2008. *Standard Test Methods for Determination of the Soil Water Characteristic Curve for Desorption Using Hanging Column, Pressure Extractor, Chilled Mirror Hygrometer, or Centrifuge, Designation: D6836*. West Conshohocken, United States. Standard Test Methods for Determination of the Soil Water Characteristic Curve for Desorption Using Hanging Column, Pressure Extractor, Chilled Mirror Hygrometer, or Centrifuge, Designation: D6836.

[46] Van Genuchten, M.T. 1980. A closed-form Equation for Predicting the Hydraulic Conductivity of Unsaturated Soils. *Soil Science Society of America Journal*. 44(5): 892–898.

[47] Leong, E.C. and H. Rahardjo. 1997. Review of Soil-Water Characteristic Curve Equations. *Journal of Geotechnical and Geoenvironmental Engineering*. 123(12): 1106–1117.

[48] Kassim, A. 2011. *Modelling the Effect of Heterogeneities on Suction Distribution Behaviour in Tropical residual Soil*. Universiti Teknologi Malaysia.

[49] Little, A.L. 1969. The Engineering Classification of Residual Tropical Soils. Proceedings of the *7th International Conference on Soil Mechanics and Foundation Engineering*. 1–10.

[50] Lee, M.L. 2008. *Influence of Rainfall Pattern on Suction Distribution and Slope Stability*. Universiti Teknologi Malaysia.

[51] Gofar, N. and M.L. Lee. 2008. Extreme Rainfall Characteristics for Surface Slope Stability in the Malaysian Peninsular. *Georisk*. 2(2): 13.

[52] Lee, L. M., N. Gofar. and H. Rahardjo. 2009. A simple model for preliminary evaluation of rainfall-induced slope instability. *Engineering Geology*. 108(3–4): 272–285.

[53] Yang, H., H. Rahardjo, B. Wibawa, and E.C. Leong. 2004. A Soil Column Apparatus for Laboratory Infiltration Study. *ASTM Geotechnical Testing Journal*. 27(4): 347–355.

[54] Rahardjo, H., A. Nio, E.C. Leong, and N. Song. 2010. Effects of Groundwater Table Position and Soil Properties on Stability of Slope during Rainfall. *Journal of Geotechnical and Geoenvironmental Engineering*. 136(11): 1555–1564.

[55] Smesrud, J. and J. Selker. 2001. Effect of Soil-Particle Size Contrast on Capillary Barrier Performance. *Journal of Geotechnical and Geoenvironmental Engineering*. 127(10): 885–888.